Erschienen in: Angewandte Chemie International Edition. Wiley. 2025, 64(2), e202414319
https://doi.org/10.1002/anie.202414319

Enzyme Mechanisms

Structures of a DNA Polymerase Caught while Incorporating Responsive Dual-Functional Nucleotide Probes

Pulak Ghosh, Karin Betz, Cédric Gutfreund, Arindam Pal, Andreas Marx, and Seergazhi G. Srivatsan**

Abstract: Functionalizing nucleic acids using DNA polymerases is essential in biophysical and biotechnology applications. This study focuses on understanding how DNA polymerases recognize and incorporate nucleotides with diverse chemical modifications, aiming to develop advanced nucleotide probes. We present the crystal structures of ternary complexes of *Thermus aquaticus* DNA polymerase (KlenTaq) with C5-heterocycle-modified environment-sensitive 2′-deoxyuridine-5′-triphosphate (dUTP) probes. These nucleotides include SedUTP, BFdUTP and FBFdUTP, which bear selenophene, benzofuran and fluorobenzofuran, respectively, at the C5 position of uracil, and exhibit high conformational sensitivity. SedUTP and FBFdUTP serve as dual-app probes, combining a fluorophore with X-ray anomalous scattering Se or ^{19}F NMR labels. Our study reveals that the size of the heterocycle influences how DNA polymerase families A and B incorporate these modified nucleotides during single nucleotide incorporation and primer extension reactions. Remarkably, the responsiveness of FBFdUTP enabled real-time monitoring of the binary complex formation and polymerase activity through fluorescence and ^{19}F NMR spectroscopy. Comparative analysis of incorporation profiles, fluorescence, ^{19}F NMR data, and crystal structures of ternary complexes highlights the plasticity of the enzyme. Key insight is provided into the role of gatekeeper amino acids (Arg660 and Arg587) in accommodating and processing these modified substrates, offering a structural basis for next-generation nucleotide probe development.

Introduction

The ability of native and engineered DNA polymerases to accept and faithfully process chemically functionalized nucleotide analogs has become a method of choice in several biotechnological applications, including contemporary nucleic acid sequencing techniques, diagnosis, bioconjugation strategies and combinatorial nucleic acid selection procedures.[1–15] These enzymes are also used to access probe-functionalized nucleic acids to study their structure, recognition and therapeutic potential.[16–27] Notably, thermostable DNA polymerases from A-family (e.g., KlenTaq) and B-family (e.g., *Thermococcus kodakarensis* (KOD)) exhibit good substrate tolerance for C5-modified pyrimidine and 7-deaza-modified purine nucleotide analogs, and hence, are widely used.[28–34] In particular, environment-sensitive fluorescent nucleotide probes, derived by conjugating or fusing heterocycles to nucleobases, represent an important class of biophysical tool to study nucleic acids.[35–47] While many of these structurally different substrates are processed by DNA polymerases with varying specificity and incorporation efficiency, currently available data does not provide an adequate understanding of the underlying mechanism that enables the enzyme to accept such unnatural nucleotides. Hence, predicting substrate tolerance remains a major challenge. In this context, we sought to establish a biochemical and biophysical platform that would allow us to correlate the binding events in the catalytic cycle and ensuing enzyme activity in real-time in solution and at atomistic level. Such an experiment will provide mechanistic insights into (i) how the enzyme interacts with nucleotide analogs and (ii) the elements that play key roles in accommodating and processing the modification, thereby enabling the design of next generation nucleotide probes.

For this purpose, we relied on crystallization experiments, configured to capture ternary complexes composed of DNA polymerase, primer-template duplex and nucleotide analogs ready for catalysis (Figure 1A).[48–50] Notably, KlenTaq has been employed as a model system to obtain structural insights into the processing of a few C5- and C7-modified pyrimidine and purine nucleotide analogs.[49–51] Further, we realize that the environment around the nucleotide analog, when bound to the enzyme active site before the reaction, after the reaction and extension, and release of modified duplex from the enzyme, would be different due to changes in local conformation and interaction partners (Figure 1B). Therefore, we wanted to leverage the microenvironment sensitivity of C5-heterocycle-modified dUTP substrates to probe the chemical space tolerance of the enzyme and simultaneously obtain real-time spectral readouts to study the individual events of the catalytic cycle. In this direction, we developed a series of

[*] Dr. P. Ghosh, A. Pal, Prof. Dr. S. G. Srivatsan
Department of Chemistry
Indian Institute of Science Education and Research (IISER), Pune,
Dr. Homi Bhabha Road, Pune 411008, India
E-mail: srivatsan@iiserpune.ac.in
Dr. K. Betz, C. Gutfreund, Prof. Dr. A. Marx
Department of Chemistry
Konstanz Research School Chemical Biology, University of Konstanz, Universitätsstraße 10, 78457, Konstanz, Germany
E-mail: andreas.marx@uni-konstanz.de

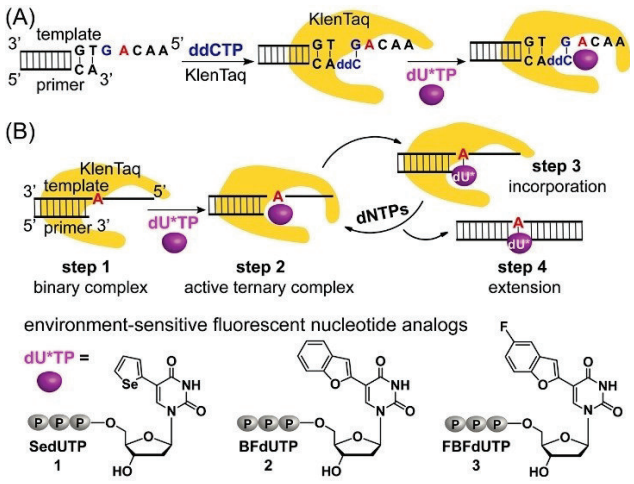

Figure 1. A) A diagram showing the crystallization setup to trap a modified nucleotide in the active ternary complex. B) Catalytic steps of the enzymatic incorporation. Chemical structures of nucleotide analogs used in this study.

fluorescent 2′-deoxyuridine (dU) analogs namely, SedU, BFdU and BTdU by conjugating selenophene, benzofuran and benzothiophene, respectively, at the C5 position of the nucleobase. These analogs serve as excellent probes in investigating the structural polymorphism of G-quadruplexes and i-motifs, and ligand-induced conformational changes in therapeutically relevant nucleic acid motifs.[52–55] More recently, we identified that the 2′-deoxynucleotide version of these nucleoside probes are efficiently incorporated into ONs by KlenTaq and KOD DNA polymerases, albeit with differences in incorporation efficiency and pattern.[56] A crystal structure of the ternary complex with KlenTaq and BFdUTP revealed the interactions between the protein and the nucleotide in the active site. While the triphosphate component of BFdUTP maintains necessary contacts for the phosphodiester bond formation, the "gatekeeper" amino acid residues, Arg660 and Arg587, adopt an alternate conformation, forming a crevice to accommodate the benzofuran moiety. However, with one structure we could not survey the chemical space tolerance of the enzyme and obtain a generalized view of how the enzyme processes smaller versus larger heterocycle-modified nucleotides.

Filling this limited understanding, we report here the crystal structures of ternary complexes of KlenTaq DNA polymerase with SedUTP, BFdUTP and FBFdUTP, which bear progressively increasing chemical modifications. Although family A (KlenTaq) and family B (KOD) DNA polymerases accept these nucleotides very well, they show differences in fidelity and incorporation efficiency in single nucleotide incorporation and primer extension (PEX) reactions. Notably, we used the remarkable environment-sensitivity of FBFdUTP, containing a fluorophore and a ^{19}F label, to monitor the binding events and enzyme activity in real-time by fluorescence and ^{19}F NMR. Importantly, by combining the insights obtained from X-ray crystal structures with biochemical and biophysical data, we now understand how the enzyme's plasticity, involving Arg660 and Arg587 as key determinants, and a balance between the size of the heterocycle modification and the additional stacking interaction it provides in the active site, combinedly orchestrates the recognition process and modulates the incorporation efficiency.

Results and Discussion

Our recent studies indicate that KlenTaq incorporates a single modified nucleotide (both SedUMP and BFdUMP) in PEX reactions with comparable efficiency as dTMP.[56] However, with templates that code for multiple insertions of modified nucleotides, it efficiently uses SedUTP to produce full-length products but fails to incorporate the bulkier nucleotide with a benzofuran modification. On the other hand, KOD, which belongs to the B-family, performs well in both single and multiple incorporation experiments, regardless of the size of the heterocycle. The structure of BFdUTP-duplex-KlenTaq complex revealed space for further expansion of the benzofuran ring that could be tolerated by the enzyme. With this basic understanding, we built an environment-sensitive congener of BFdUTP by integrating a fluorine atom into the BF core (FBFdUTP **3**). The introduction of a ^{19}F label gives two main advantages in addition to a high gyromagnetic coefficient, 100 % natural abundance, and high sensitivity to changes in the local environment.[57,58] FBFdUTP is composed of a fluorophore and a ^{19}F NMR isotope opening up a two-channel spectroscopic system to monitor the catalytic events under equilibrium conditions. Since both probe components are integrated in the same electronic environment, the data obtained from fluorescence and NMR experiments can be efficiently correlated with each other and with the crystal structure.

Enzymatic Incorporation of FBFdUMP into ONs

FBFdUTP **3** was prepared by reacting FBFdU (**3b**)[59,60] with $POCl_3$ and then with *bis*-tributylammonium pyrophosphate (Scheme S1). The ability of FBFdUTP to act as a dTTP analog was tested by performing PEX reactions using KlenTaq and KOD DNA polymerases. A 5′-FAM-modified primer **P1** was hybridized to a set of templates (**T1**–**T5**), which code for the incorporation of the respective mononucleotides into the nascent DNA strand at various positions including the start site, a location away from the start site, and at multiple positions (Table 1, Figure 2A). In reactions conducted with templates **T1** and **T2** guiding a single modification, KlenTaq accepted the modified nucleotide with comparable efficiency to the natural dTTP, resulting in the formation of respective full-length products (Figure 2B, lanes 4, 5 and 7, 8). Reactions in the absence of dTTP/**3** but in the presence of other dNTPs did not yield the full-length product, indicating that the incorporation of FBFdUMP is not due to a misincorporation (Figure 2B, lanes 3 and 6). KlenTaq failed to produce modified full-length products with **T3** and **T4** designed to incorporate two

Table 1: Sequence of ONs used in this study.[a]

ONs	Sequence
P1	5′ FAM-GTGGTGCGAAATTTCTGACAGACA 3′
T1	3′ CACCACGCTTTAAAGACTGTCTGT**A**CTGTCTGCGTG 5′
T2	3′ CACCACGCTTTAAAGACTGTCTGTGCTGTCT**A**CGTG 5′
T3	3′ CACCACGCTTTAAAGACTGTCTGTGCTGT**AT**ACGTG 5′
T4	3′ CACCACGCTTTAAAGACTGTCTGTGCTGTCT**AA**GTG 5′
T5	3′ CACCACGCTTTAAAGACTGTCTGTGCTGT**AT****AA**GTG 5′
P2	5′ FAM-GGAGCTCAGCCTTCACTGC 3′
P3	5′ GGAGCTCAGCCTTCACTGC 3′
T6	3′ CCTCGAGTCGGAAGTGACG**A**CGATTTGATATAACGAT CGCGTG 5′
P2*	5′ FAM-GGAGCTCAGCCTTCACTGC-**FBFdU** 3′
P3*	5′ GGAGCTCAGCCTTCACTGC-**FBFdU** 3′
P4	5′ GACCACGGCCA 3′
T7	3′ CCTCGAGTCGGAAGTGACGATGTCGCTCCGCGTC 5′
T8	3′ CTGGTGCCGGT**GA**CAA 5′
P5	5′ GGAGCTCAGCCTTCACTGddC 3′
P6	5′ FAM-GACCACGGCCAC 3′

[a] The incorporation of modified nucleotide analogs in PEX and single nucleotide incorporation assays is guided by dA(s), highlighted in red in template strands. In ON **T8**, during crystallization trials, the termination of the extension was achieved by incorporating ddCMP opposite dG marked in blue.

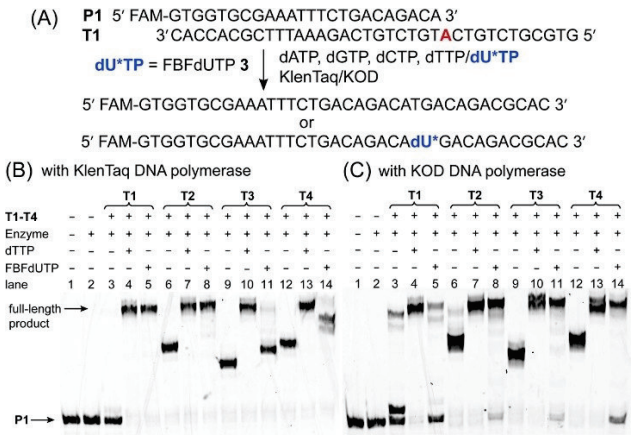

Figure 2. A) Scheme showing the incorporation of FBFdUMP by PEX reactions using DNA polymerases. B,C) Incorporation of FBFdUMP using KlenTaq and KOD DNA polymerases, respectively, in the presence of primer **P1** and templates **T1**–**T4**. For reactions with **T5** see Figure S1.

modifications (Figure 2B, lanes 11 and 14). In contrast, KOD DNA polymerase efficiently processed FBFdUTP in the presence of all the templates (**T1**–**T5**), generating respective modified oligonucleotide (ON) products comparable to those formed in the presence of dTTP (Figure 2C, and Figure S1, lanes 8 and 9). We observe that introducing a fluorine label in the benzofuran ring does not impair its incorporation efficiency by DNA polymerases. While KOD is suitable for multiple labeling, KlenTaq shows difficulties in incorporating FBFdUMP in the presence of high demanding templates. These observations concur with the results obtained in our previous study using BFdUTP (see above).[56]

Site-specifically ^{19}F-labeled ONs serve as powerful tools to probe nucleic acid secondary structures, nucleic acid-protein and drug interactions.[59–69] These ONs are typically obtained by the solid-phase ON synthesis method. Here, we wanted to establish a method to introduce FBFdU site-specifically into ONs using DNA polymerases (Figure S2A).[70–72] A primer-template duplex (**P2**·**T6**) was reacted with FBFdUTP in the presence of KlenTaq or KOD to incorporate a single modified nucleotide at the 3′-end of the primer. While KOD DNA polymerase produced largely a double-modified product due to the misincorporation of FBFdUMP, KlenTaq specifically added only one modification at the 3′-end of **P2** (Figure S2B). Therefore, using the high fidelity of KlenTaq, a single FBFdUMP was incorporated into **P2** in the first step (Figure S2C, lane 2). The labeled ON **P2*** was then precipitated using 70 % ethanol and the extension step was carried out by adding natural dNTPs and KlenTaq or KOD. In the second step, both the enzymes efficiently extended the modified duplex to produce site-specifically labeled ON product **P2**** (Figure S2C, lanes 4 and 6). Identity of **P2*** and **P2**** was confirmed by mass spectrometry (Table S1 and Figure S3). Thus, a judicious choice of enzyme in the first and second step successfully produces site-specifically functionalized DNA ONs.

Probing Complex Formation and Enzymatic Incorporation by Fluorescence and ^{19}F NMR Spectroscopy

Photophysical properties of FBFdU are highly sensitive to its surrounding polarity and viscosity due to the presence of a rotatable aryl-aryl bond between FBF and uracil rings (Table S2).[59] For example, in a polar environment or in a scenario resulting in the rigidification of the fluorophore it shows a red-shifted intense emission band (437 nm). Whereas, in non-polar and stacked environments it displays a blue-shifted weak emission band. Further, the nucleoside exhibits distinct ^{19}F chemical shifts in solvents of different polarity and viscosity.[59] Basic photophysical and ^{19}F NMR analyses of FBFdUTP in different solvents reveal a trend similar to the nucleoside (Figure S4 and Table S3). Therefore, we tested its proficiency to serve as a probe to monitor the binding processes and DNA polymerase activity by fluorescence and ^{19}F NMR.

In the PEX reaction, the open conformation of a binary complex of enzyme and primer-template duplex allows the incoming nucleotide to bind to the active site resulting in a closed conformation.[73,74] Once the phosphodiester linkage is formed with the modified nucleotide, the binary complex opens up and allows the next nucleotide to bind and extend the DNA chain (Figure 1B). For these events to be monitored FBFdU should exhibit distinct spectral signals (Figure 3A). A primer-template duplex formed by hybridizing 3′-FBFdU-modified primer **P3*** and **T7** displayed a blue-shifted (λ_{em} = 420 nm) and a very weak fluorescence band (Figures 3B and 3 C). This is because the base-paired analog in the duplex is in a less polar environment (similar to methanol, Table S3) and experiences partial stacking

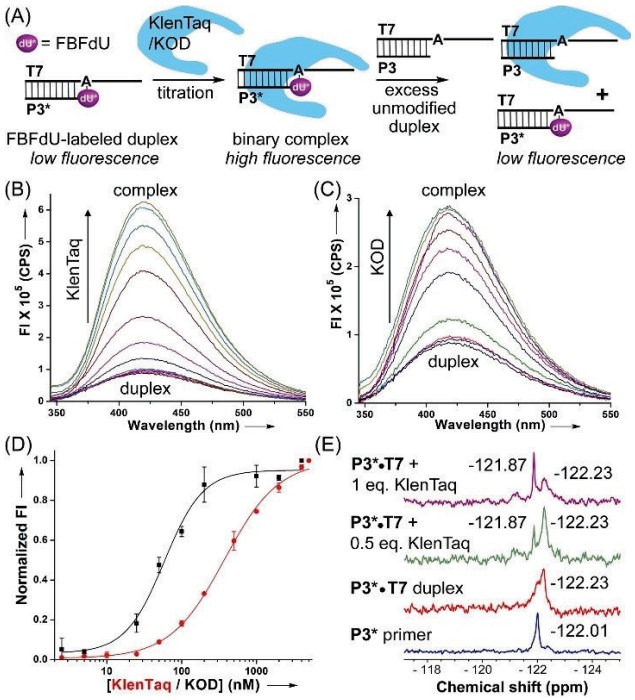

Figure 3. A) Scheme for monitoring the binary complex formation. B,C) Fluorescence spectra for the duplex **P3*·T7** (50 nM) with increasing concentrations of KlenTaq and KOD DNA polymerase, respectively (0–5 μM). D) Curve fits for the binding of KlenTaq and KOD to the duplex. Normalized FI at λ_{em} (420 nm) was plotted against the concentration of enzymes. Values are plotted as a mean ± s.d for $n = 3$ independent experiments. E) ^{19}F NMR spectra of **P3***, primer-template duplex **P3*·T7** and duplex with increasing equivalents of KlenTaq. See the Supporting Information for experimental details.

interaction with the neighboring base. When the modified duplex **P3*·T7** was incubated with increased concentrations of KlenTaq and KOD, it showed a significant increase in the fluorescence intensity (FI) with negligible changes in the emission maximum (Figures 3B and 3C). The enhanced fluorescence exhibited by the enzyme-duplex binary complex is likely due to the rigidification of the fluorophore in the enzyme pocket. A plot of normalized FI versus enzyme concentration gave an apparent K_d of 0.36 ± 0.01 μM for KlenTaq and 0.06 ± 0.02 μM for KOD (Figure 3D). Stronger binding exhibited by KOD may have in part manifested in better incorporation of the nucleotide analog as compared to KlenTaq with different templates. To prove the specific binding of the modified duplex to the enzymes, we performed a competitive displacement assay. A binary complex (**P3*·T7** duplex 50 nM and KlenTaq/KOD 1 μM) was prepared, which exhibits saturation FI. Titration with increasing concentrations of an unlabeled DNA duplex (**P3·T7**) resulted in a gradual reduction in the fluorescence due to the displacement of a less emissive duplex **P3*·T7** from the enzyme active site (Figure S6). Note that even a 20-fold excess of the unmodified duplex did not show complete dissociation, indicating that the modified duplex forms a stable complex with both enzymes. Electrophoretic mobility shift assay under non-denaturing conditions also confirmed the formation of stable binary complexes with both the enzymes (Figure S7).

Next, we designed a fluorescence method to detect the polymerase activity (Figure 4A). FBFdUTP in the reaction buffer displayed an intense fluorescence band centered around 437 nm (black dashed line, Figures 4B and 4C). Adding FBFdUTP to the primer-template duplex (**P3·T7**) or polymerases alone showed no changes in fluorescence, indicating that it does not interact with the duplex or enzyme directly. Rewardingly, when FBFdUTP was added to samples of a binary complex (enzyme plus **P3·T7**), each containing increasing concentrations of KlenTaq or KOD DNA polymerase, a significant decrease in fluorescence accompanied by a blue shift in the emission maximum (λ_{em} = ~420 nm) was observed (orange dashed line). In a control experiment, a binary complex made of KlenTaq/KOD and a 3′-ddC-modified primer-template duplex **P5·T7** was added to FBFdUTP. Due to the presence of a blocked 3′-end, there was no incorporation, and thus, no decrease in FI was observed (Figure 4B and 4C, green dashed line). Therefore, the observed outcome is because of the incorporation of a single FBFdUMP at the 3′-end of the primer resulting in the generation of a less emissive free FBFdU-labeled duplex **P3*·T7** and or labeled duplex bound to the enzyme (Figure 4A). The species responsible for showing low fluorescence was determined by ^{19}F NMR (*vide infra*). Reactions analyzed by PAGE under similar conditions confirmed the incorporation of a single FBFdUMP at the primer end by both the enzymes (Figure S8). It is to be noted that the formation of a ternary complex was not evident as the fluorescence of the free nucleotide probe and when bound to the binary complex was very similar (Figure 4B and 4C, compare black and green dashed lines).

Interestingly, we were able to detect the formation of binary and ternary complexes and enzyme activity in solution by ^{19}F NMR using the responsiveness of FBFdUTP. FBFdU-modified primer **P3*** in KlenTaq binding buffer exhibited a peak at −122.01 ppm (Figure 3E, blue trace). When hybridized to its complementary ON **T7**, the signal for the duplex slightly shifted to −122.23 ppm (Figure 3E, red trace). Upon addition of increasing equivalents of KlenTaq, a new peak at −121.87 ppm corresponding to the binary complex appeared with a concomitant decrease in the duplex peak (Figure 3E, green and purple traces). Interestingly, even when the sample was heated at 95 °C for 20 min, no discernible change in peak intensity at −121.87 ppm was observed, suggesting the superior stability of the complex even at an elevated temperature (Figure S9B). Furthermore, a mixture of KlenTaq, **P5·T7** duplex and FBFdUTP gave a signal at −121.24 ppm, distinct from the nucleotide analog (−122.36 ppm), thereby enabling the detection of the ternary complex formation in solution (Figure S10A). Using these distinct ^{19}F signatures, we next studied the incorporation of the nucleotide analog. The free nucleotide FBFdUTP showed a sharp peak at −122.36 ppm (Figure 4D, cyan trace). Upon addition of FBFdUTP to a binary complex formed by mixing unmodified duplex (**P3·T7**) and KlenTaq, the peak for the substrate diminished and a new peak corresponding to the single nucleotide incorporated

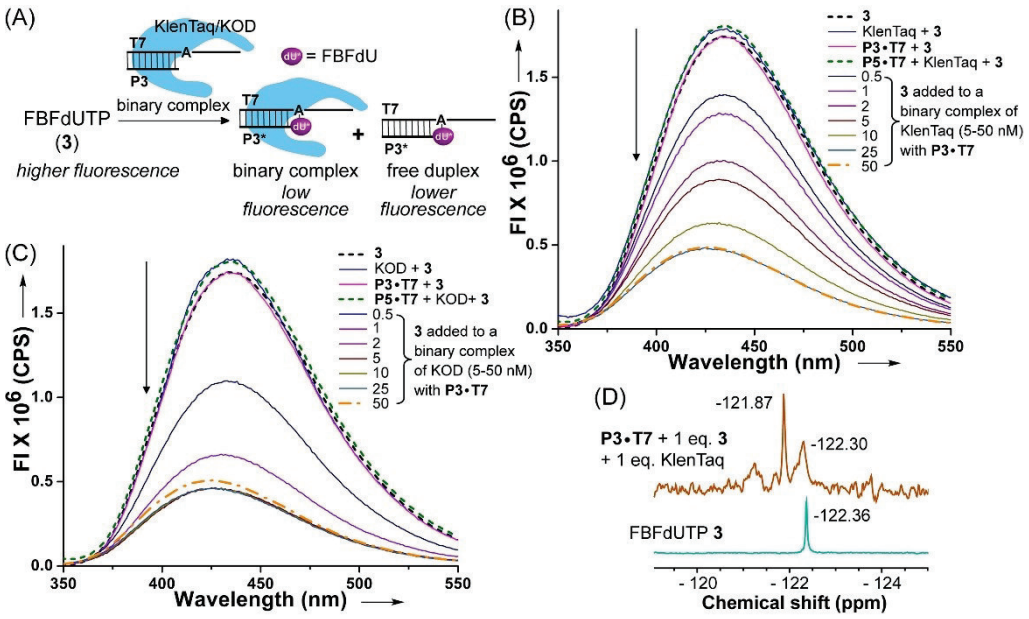

Figure 4. A) Scheme for monitoring the incorporation activity of DNA polymerases. B, C) Fluorescence spectra showing the incorporation of mononucleotide of FBFdUTP by KlenTaq and KOD DNA polymerases, respectively. Colored lines represented in half parenthesis denote the concentration of enzymes used. Values are plotted as a mean of $n = 2$ independent sample measurements. D) Incorporation process as monitored by ^{19}F NMR spectroscopy. See the Supporting Information for experimental details.

product bound to the enzyme appeared at −121.87 ppm (Figure 4D, brown trace). This peak exhibits the same chemical shift found for the **P3***·**T7**-KlenTaq complex (compare with purple trace, Figure 3E). These results indicate that after incorporation, the labeled duplex largely stays in the bound state, and hence, progressive quenching in the emission intensity observed during FBFdUMP incorporation is due to the formation of the less emissive **P3***·**T7**-enzyme complex (*vide supra*). The binding of KOD to the duplex did not produce a well-resolved peak to detect the binary complex or reaction unambiguously (Figure S10B). Taken together, our probe provides an efficient two-channel spectroscopic read out to detect the binding events and monitor the enzyme activity. To gain further understanding at the atomic level, we relied on X-ray crystallography to obtain structures of ternary complexes of DNA polymerases with the nucleotide analogs.

X-ray Crystal Structures of Ternary Complexes Provide Insights into the Incorporation Mechanism

A snapshot of the catalytic step in which the nucleotide analog is poised for incorporation was obtained by setting up crystallization experiments with SedUTP and FBFdUTP in the presence of KlenTaq and KOD DNA polymerases (Figure 1A). We used **T8** template configured to incorporate ddCMP as the first nucleotide and modified analogs as the second nucleotide to primer **P4** (Table 1). A reaction primed with ddCMP stops the polymerization and enables the capture of nucleotide analogs in the active site aligned for catalysis. Unfortunately, with KOD, we only obtained microcrystals, which did not provide quality diffraction data. Rewardingly, high-resolution structures of KlenTaq ternary complexes composed of SedUTP (2.6 Å, Figure S11A) and FBFdUTP (2.1 Å, Figure S11C) in the nucleotide-binding site were obtained (Table S4). Superimposition of structures reveals that complexes with SedUTP and FBFdUTP adopt a structure that closely resembles the complex containing a natural nucleoside triphosphate (PDB: 3RTV)[75] (Figure S11B and S11D). The RMSD value for Cα atoms is 0.499 Å and 0.491 Å (for each 540 residues aligned compared to 3RTV), respectively. In the ternary complexes composed of SedUTP, BFdUTP (PDB: 7OWF)[56] and FBFdUTP, the finger region adopts a closed conformation, and the O helix aligns atop the nucleotide bound in the active site much like in the structure with dCTP (Figure 5A–5D). The nucleotide analogs form a Watson–Crick base pair with the dA of the template strand and also partially stack with ddCMP inserted at the primer 3′-end (see also Figure S12). Selenophene, benzofuran, and fluorobenzofuran moieties are somewhat non-coplanar with respect to the uracil ring (Figure S13).

Further analysis of individual structures provided insights into the conformational differences in the active site that leads to the accommodation of nucleotides based on the size of the heterocycle modification. In the presence of SedUTP, two key amino acid residues, Arg587 and Arg660 adopt a conformation similar to the structure obtained with a native nucleotide (Figure 6A and 6B). This indicates that SedUTP fits well in the KlenTaq pocket preserving the interaction network of Arg587 and Arg660 with the neighboring residues and the primer strand. Further, the Se atom upon X-ray irradiation produced very good anomalous

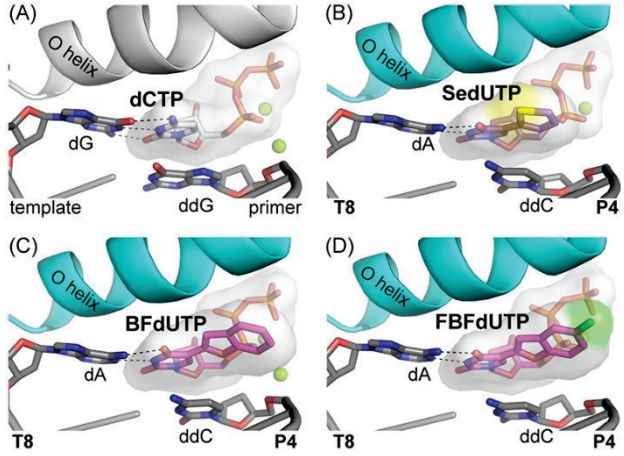

Figure 5. Close-up views of the active site showing the bound nucleotide. A) dCTP, B) SedUTP, C) BFdUTP and D) FBFdUTP. The Watson–Crick base pairing between nucleotide analogs and dA of the **T8** strand is indicated with dashed lines. SedUTP is shown in purple, and BFdUTP and FBFdUTP are shown in magenta. Se and F atoms are shown in yellow and green, respectively.

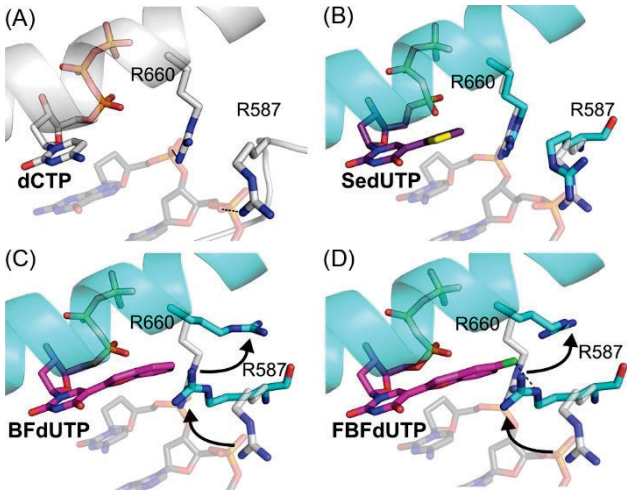

Figure 6. Superimposed structures with native (gray; PDB: 3RTV) and modified nucleotides highlighting the differences in the orientation of Arg660 and Arg587 residues. A) dCTP, B) SedUTP (purple), C) BFdUTP (magenta) and D) FBFdUTP (magenta). Se and F atoms are shown in yellow and green, respectively. Shifts for Arg660 and Arg587 residues as compared to the natural structure are highlighted with arrows. Potential interactions mentioned in the text are shown as black dashed lines.

scattering signals that could be utilized in phasing by either SAD or MAD techniques (see anomalous map for Se in Figure S13D).[55,76–78] To accommodate FBFdU, Arg660 and Arg587 assume an alternate conformation as compared to the structure in the presence of a natural nucleotide but similar to BFdUTP (Figure 6C and 6D). Typically, in closed ternary KlenTaq structures, Arg660 points towards the primer 3′-terminus, where it could interact with the phosphate backbone via a hydrogen bond and might stabilize the closed active state of the enzyme (Figure 6A).[48–50,79,80] Arg587 usually also points towards the primer strand and can interact with the phosphate group of the 2nd primer nucleotide. In the SedUTP structure, Arg660 can interact with the primer terminus (distance 2.5 Å) just as in the natural case. However, in the KlenTaq-FBFdUTP structure, Arg660 flips out and makes room to accommodate the bulkier FBF modification (see arrows in Figure 6D). During this process, Arg587 comes closer to the FBF ring and the primer terminus where it could engage interactions. It is to be noted that due to the highly polarized nature of the C–F bond and the presence of the vacant σ*C–F orbital, the fluorine atom can potentially engage in dipole-dipole and charge-dipole interactions with adjacent electropositive centers, lone pairs or electron rich bonds.[81,82] Notably, such interactions have been reasoned to play a prominent role in the ability of DNA polymerases to process fluorinated nucleotide analogs.[83–85] In the structure of KlenTaq-FBFdUTP, we observe that the fluorine atom of FBF is in close proximity to Arg660 and Arg587 residues (2.9 Å to 3.2 Å, Figure S14). In particular, it comes closer to the guanidinium group of Arg587 (2.9 Å), which together may have helped in positioning the nucleotide in the pocket (Figure 6D and Figure S14). This alternate conformation produces a cleft to encase the heterocycle modification in the active site (Figure S15A). As envisioned, based on the structure with BFdUTP, KlenTaq does have room to accommodate the fluorine-expanded heterocycle in its pocket, thereby incorporating both the nucleotides in a similar fashion (Figure S15A and S15B).

In all the structures, we observe additional stacking interactions between the heterocycle moieties and the 3′-end ddC of the primer strand, albeit small differences in the extent of interaction (Figure S12). However, this seems not to affect the active site conformation as compared to the steric hindrance posed by larger heterocycles namely, BF and FBF, which results in the reorientation of Arg660 and Arg587 residues. Despite these differences, interactions between the enzyme and triphosphate part of the nucleotide, as well as the distance between the C3′ of the primer end and α-phosphorus of the nucleotide, necessary for the phosphodiester bond formation are very similar in structures with SedUTP (4.1 Å), BFdUTP (3.8 Å),[56] FBFdUTP (3.8 Å) and dCTP (3.9 Å, Figure S16A–S16D).[75] Compared to the natural complex and the BFdUTP-bound structure, only one instead of two magnesium ions is bound in the active site of KlenTaq-SedUTP and KlenTaq-FBFdUTP (Figure 5). The reason for this difference is still unclear and we assume that it is not modification-specific. The aspartate residues (Asp610 and Asp785) that normally coordinate the second magnesium ion actually overlap well in all four structures (Figure S16E–S16H). Taken together, these results illustrate the ‘elegance’ of the enzyme as it uses different mechanisms to accommodate heterocycle groups based on their size, while modifications by themselves do not alter the basic alignment of the sugar and triphosphate moieties in the enzyme pocket to enable the incorporation process.

Correlating Structures with Primer Extension Process Employing Different Templates

The primer-template duplex encased in the groove formed by the thumb and palm domains of KlenTaq assumes A-form helical geometry near the active site characterized by a narrow major grove (Figure S17A).[75] The enzyme channel that spans the duplex is also narrow (Figure S17C). Further, the tip of the thumb that interacts with the primer strand houses a loop formed by residues 506–509, which hovers over the primer phosphate backbone. This loop extends towards the major groove side. Similar structural features are exhibited by all three KlenTaq-nucleotide analog complexes (Figure S17E–S17 J). It is to be noted that the heterocycle moiety conjugated at the C5-position of pyrimidine, when incorporated into a duplex, would be projected in the major groove. Based on the incorporation data, and mechanism of incorporation presented above, once a single modified mononucleotide analog is added to the primer, subsequent addition of natural nucleotides is possible. Hence, the successful formation of full-length products with templates **T1** and **T2** is achieved, as singly modified primers did not impede their translocation along the channel. However, the reaction efficiency depended on the size of the modification when ONs **T3**–**T5** templating for two or more modifications in the primer strand were used. KlenTaq efficiently incorporated the smaller-sized SedUMP at multiple sites as the recognition mechanism is similar to the natural nucleotide. Further, we believe that loop residues 506–509 are flexible enough to pass multiple smaller nucleotide analogs. In the case of consecutive addition of bulkier nucleotide analogs (BFdUTP and FBFdUTP), Arg660 and Arg587 residues must repeatedly adopt alternate conformations, which could potentially exert more pressure on the enzyme so that the PEX reaction results in the formation of truncated ON products.[80] Furthermore, we speculate that the loop hovering over the major groove could impede the translocation of primers containing multiple bulky modifications projected in that groove. The KOD structure, on the other hand, features a B-form duplex with a wider major groove and larger channel volume (Figure S17B and S17D).[86] An equivalent loop formed by the tip of the thumb (residues 668–675) drifts over the minor groove only (Figure S17D). Due to these structural features, we believe that KOD efficiently allows single as well as multiple insertions of all the tested nucleotide substrates efficiently.

To further corroborate the impact of heterocycle modification on the incorporation efficiency, we performed a competition assay between dTTP and modified nucleotides (Figure S18A). Different molar ratios of modified nucleotides and dTTP were subjected to a single nucleotide incorporation assay in the presence of KlenTaq and **P6**·**T8** duplex. Due to the slower mobility of modified ON products as compared to a dTMP-added product, two well-separated bands were obtained that could be quantified individually (Figure S18B–S18D). Reactions with BFdUTP and FBFdUTP required nearly 35/1 of dU*TP:dTTP to afford equal amounts of singly added products, suggesting that the enzyme has a higher preference for dTTP (Figure S18E and S18F). Interestingly, in the presence of SedUTP, nearly 15 equivalents of dTTP were required to produce equally modified products (Figure S18G). This observation along with PEX results indicate that SedUTP is better accepted by the enzyme as compared to the natural and heterobicycle-modified nucleotides. Two factors could potentially attribute to this outcome. (I) The incoming nucleotide triphosphate partially stacks with the primer 3′-end nucleotide and the extent of stacking may have some influence on the incorporation efficiency and (II) bulkier modifications alter the original conformation of Arg660 and Arg587 residues (Figures 5 and 6), which most probably leads to impaired incorporation. Even if additional stacking with the primer end is possible for BFdUTP and FBFdUTP, the second point probably prevails here. In contrast, SedUTP fits well in the enzyme pocket like dTTP, but imparts additional stacking interaction without affecting the conformation of Arg660 and Arg587 residues, which may explain its superior substrate properties. We then evaluated the effect of C5-modification on KlenTaq kinetics in single nucleotide incorporation reactions[87,88] using **P1**·**T1** duplex and dTTP/SedUTP/FBFdUTP. The initial velocity (V_i) for the incorporation of the natural nucleotide ($dTTP = 0.70 \pm 0.03\ s^{-1}$) was found to be noticeably lower as compared to the incorporation of the nucleotide analogs ($SedUTP = 1.58 \pm 0.06\ s^{-}$; $FBFdUTP = 1.22 \pm 0.06\ s^{-1}$) (Figure S19). These preliminary results suggest that our C5-heterocycle-modified nucleotide analogs are incorporated faster compared to the native nucleotide by the enzyme. However, the type of nucleobase (pyrimidine/purine/modified nucleotide) at the 3'-end of the primer, and templates that would direct the insertion of nucleotide analogs near and away from the start site and at multiple sites could have ramifications on the kinetics of incorporation. As a follow-up of this work, we intend to carry out a rigorous kinetic analysis on these factors using different nucleotides, primers and templates.

Conclusions

In summary, we gained a comprehensive understanding of the processing of environment-sensitive nucleotide probes by DNA polymerases that are widely used in current applications. Biochemical evaluation revealed that C5-heterocycle-modified nucleotides are differentially incorporated by A-family (KlenTaq) and B-family (KOD) DNA polymerases. KlenTaq exhibited superior fidelity and stringency in processing the nucleotides based on the size of the heterocycle, whereas KOD incorporated nucleotide analogs at single and multiple sites efficiently regardless of the heterocycle size. In addition, FBFdUTP serves as an excellent probe to analyze catalytic events under equilibrium conditions by fluorescence and ^{19}F NMR techniques. Crystals of ternary complexes obtained in the presence of all three nucleotides provided a progressive insight into how KlenTaq uses its flexible amino acid residues to accommodate and process a smaller and a larger modified nucleotide. These findings further expand the limited knowledge on the

interplay between the polymerases and chemically diverse substrates, and build a basis for developing nucleotide probes for advanced applications.

Supporting Information

Supporting Information is available online.

Acknowledgements

P.G. is thankful to IISER Pune for the graduate research fellowship. A.P. is grateful to PMRF, India for a graduate research fellowship. We thank Sarupa Roy for helping us with ^{19}F NMR experiments. The synchrotron X-ray data was collected at beamline P13 operated by EMBL Hamburg at the PETRA III storage ring (DESY, Hamburg, Germany). We thank Dr. Gleb Bourenkov and Dr. Isabel Bento for their assistance in using the beamline. S.G.S. is grateful to the Alexander von Humboldt-Foundation for a renewed research fellowship. This work was supported by a SERB grant (CRG/2022/000284) to S.G.S. and A.M. gratefully acknowledges funding by the Deutsche Forschungsgemeinschaft (DFG, MA 2288/22-1).

Conflict of Interest

The authors declare no conflict of interest.

The data that support this study are available in the Supporting Information of this article. The atomic coordinates and structure factors are deposited on the Protein Data Bank with accession code 9FM3 for KlenTaq-SedUTP and 9FMF for KlenTaq-FBFdUTP, respectively.

Keywords: DNA polymerases · fluorescent nucleotide probes · ^{19}F NMR spectroscopy · nucleosides · X-ray crystallography

[1] D. R. Bentley, et al. *Nature.* **2008**, *456*, 53–59.
[2] M. L. Metzker, *Nat. Rev. Genet.* **2010**, *11*, 31–46.
[3] L. Tan, Y. Liu, Q. Yang, X. Li, X.-Y. Wu, B. Gong, Y.-M. Shen, Z. Shao, *Chem. Commun.* **2016**, *52*, 954–957.
[4] S. Goodwin, J. D. McPherson, W. R. McCombie, *Nat. Rev. Genet.* **2016**, *17*, 333–351.
[5] J. Aschenbrenner, A. Marx, *Curr. Opin. Biotechnol.* **2017**, *48*, 187–195.
[6] M. Hocek, *Acc. Chem. Res.* **2019**, *52*, 1730–1737.
[7] N. Klöcker, F. P. Weissenboeck, A. Rentmeister, *Chem. Soc. Rev.* **2020**, *49*, 8749–8773.
[8] P. M. E. Gramlich, C. T. Wirges, A. Manetto, T. Carell, *Angew. Chem. Int. Ed.* **2008**, *47*, 8350–8358.
[9] M. Hollenstein, *Molecules* **2012**, *17*, 13569.
[10] X. Ren, M. Gerowska, A. H. El-Sagheer, T. Brown, *Bioorg. Med. Chem.* **2014**, *22*, 4384–4390.
[11] U. Reisacher, D. Ploschik, F. Rönicke, G. B. Cserép, P. Kele, H.-A. Wagenknecht, *Chem. Sci.* **2019**, *10*, 4032–4037.
[12] A. Shoji, M. Kuwahara, H. Ozaki, H. Sawai, *J. Am. Chem. Soc.* **2007**, *129*, 1456–1464.
[13] G. Mayer, *Angew. Chem. Int. Ed.* **2009**, *48*, 2672–2689.
[14] M. Kimoto, R. Yamashige, K. Matsunaga, S. Yokoyama, I. Hirao, *Nat. Biotechnol.* **2013**, *31*, 453–457.
[15] K. Sefah, Z. Yang, K. M. Bradley, S. Hoshika, E. Jiménez, L. Zhang, G. Zhu, S. Shanker, F. Yu, D. Turek, W. Tan, S. A. Benner, *Proc. Natl. Acad. Sci. USA* **2014**, *111*, 1449–1454.
[16] S. K. Jarchow-Choy, A. T. Krueger, H. Liu, J. Gao, E. T. Kool, *Nucleic Acids Res.* **2011**, *39*, 1586–1594.
[17] T. Chen, F. E. Romesberg, *Angew. Chem. Int. Ed.* **2017**, *56*, 14046–14051.
[18] J. Jakubovska, D. Tauraite, L. Birštonas, R. Meškys, *Nucleic Acids Res.* **2018**, *46*, 5911–5923.
[19] G. S. Ravi Kumara, Y. J. Seo, *Org. Biomol. Chem.* **2021**, *19*, 5788–5793.
[20] A. Espinasse, H. K. Lembke, A. A. Cao, E. E. Carlson, *RSC Chem. Biol.* **2020**, *1*, 333–351.
[21] R. Haslecker, V. V. Pham, D. Glänzer, C. Kreutz, T. K. Dayie, V. M. D'Souza, *Nat. Commun.* **2023**, *14*, 8422.
[22] M. Brunderová, V. Havlíček, J. Matyašovský, R. Pohl, L. P. Slavětínská, M. Krömer, M. Hocek, *Nat. Commun.* **2024**, *15*, 3054.
[23] N. Seul, D. Lamade, P. Stoychev, M. Mijic, R. T. Michenfelder, L. Rieger, P. Geng, H.-A. Wagenknecht, *Angew. Chem. Int. Ed.* **2024**, *63*, e202403044.
[24] A. A. Wilkinson, E. Jagu, K. Ubych, S. Coulthard, A. E. Rushton, J. Kennefick, Q. Su, R. K. Neely, P. Fernandez-Trillo, *ACS Cent. Sci.* **2020**, *6*, 525–534.
[25] Q. Li, V. A. Maola, N. Chim, J. Hussain, A. Lozoya-Colinas, J. C. Chaput, *J. Am. Chem. Soc.* **2021**, *143*, 17761–17768.
[26] H. Neitz, C. Höbartner, *Chem. Commun.* **2023**, *59*, 12003–12006.
[27] K. Duffy, S. Arangundy-Franklin, P. Holliger, *BMC Biol.* **2020**, *18*, 112.
[28] M. Kuwahara, J. Nagashima, M. Hasegawa, T. Tamura, R. Kitagata, K. Hanawa, S. Hososhima, T. Kasamatsu, H. Ozaki, H. Sawai, *Nucleic Acids Res.* **2006**, *34*, 5383–5394.
[29] S. Jager, M. Famulok, *Angew. Chem. Int. Ed.* **2004**, *43*, 3337–3340.
[30] F. J. Ghadessy, N. Ramsay, F. Boudsocq, D. Loakes, A. Brown, S. Iwai, A. Vaisman, R. Woodgate, P. Holliger, *Nat. Biotechnol.* **2004**, *22*,755–759.
[31] J. Gierlich, K. Gutsmiedl, P. M. E. Gramlich, A. Schmidt, G. A. Burley, T. Carell, *Chem. Eur. J.* **2007**, *13*, 9486–9494.
[32] H. Mei, J. Y. Liao, R. M. Jimenez, Y. Wang, S. Bala, C. McCloskey, C. Switzer, J. C. Chaput, *J. Am. Chem. Soc.* **2018**, *140*, 5706–5713.
[33] C. Dutson, E. Allen, M. J. Thompson, J. H. Hedley, H. E. Murton, D. M. Williams, *Molecules* **2021**, *26*, 2250.
[34] N. Kuprikova, M. Ondruš, L. Bednárová, M. Riopedre-Fernandez, L. P. Slavětínská, V. Sýkorová, M. Hocek, *Nucleic Acids Res.* **2023**, *51*, 11428–11438.
[35] N. J. Greco, Y. Tor, *J. Am. Chem. Soc.* **2005**, *127*, 10784–10785.
[36] P. Sandin, G. Stengel, T. Ljungdahl, K. Börjesson, B. Macao, L. M. Wilhelmsson, *Nucleic Acids Res.* **2009**, *37*, 3924–3933.
[37] M. Sholokh, R. Sharma, D. Shin, R. Das, O. A. Zaporozhets, Y. Tor, Y. Mély, *J. Am. Chem. Soc.* **2015**, *137*, 3185–3188.
[38] H. Yang, H. Mei, F. Seela, *Chem. Eur. J.* **2015**, *21*, 10207–10219.
[39] T. Z. Cservenyi, A. J. Van Riesen, F. D. Berger, A. Desoky, R. A. Manderville, *ACS Chem. Biol.* **2016**, *11*, 2576–2582.
[40] C. S. Eubanks, J. E. Forte, G. J. Kapral, A. E. Hargrove, *J. Am. Chem. Soc.* **2017**, *139*, 409–416.
[41] W. Xu, K. M. Chan, E. T. Kool, *Nat. Chem.* **2017**, *9*, 1043–1055.

[42] D. Dziuba, P. Jurkiewicz, M. Cebecauer, M. Hof, M. Hocek, *Angew. Chem. Int. Ed.* **2016**, *55*, 174–178.
[43] A. Karimi, R. Börner, G. Mata, N. W. Luedtke, *J. Am. Chem. Soc.* **2020**, *142*, 14422–14426.
[44] D. Wang, A. Shalamberidze, A. E. Arguello, B. W. Purse, R. E. Kleiner, *J. Am. Chem. Soc.* **2022**, *144*, 14647–14656.
[45] T. Kumagai, B. Kinoshita, S. Hirashima, H. Sugiyama, S. Park, *ACS Sens.* **2023**, *8*, 923–932.
[46] Y. Tor, *Acc. Chem. Res.* **2024**, *57*, 1325–1335.
[47] M. Kuba, P. Khoroshyy, M. Lepšík, E. Kužmová, D. Kodr, T. Kraus, M. Hocek, *Angew. Chem. Int. Ed.* **2023**, *62*, e202307548.
[48] Y. Li, G. Waksman, *Protein Sci.* **2001** *10*,1225–1233.
[49] S. Obeid, A. Baccaro, W. Welte, K. Diederichs, A. Marx, *Proc. Natl. Acad. Sci. USA* **2010**, *107*, 21327–21331.
[50] A. Hottin, K. Betz, K. Diederichs, A. Marx, *Chem. Eur. J.* **2017**, *23*, 2109–2118.
[51] K. Bergen, A. L. Steck, S. Strütt, A. Baccaro, W. Welte, K. Diederichs, A. Marx, *J. Am. Chem. Soc.* **2012**, *134*, 11840–11843.
[52] A. A. Tanpure, S. G. Srivatsan, *Chem. Eur. J.* **2011**, *17*, 12820–12827.
[53] A. A. Tanpure, S. G. Srivatsan, *Nucleic Acids Res.* **2015**, *43*, e149.
[54] A. Nuthanakanti, M. A. Boerneke, T. Hermann, S. G. Srivatsan, *Angew. Chem. Int. Ed.* **2017**, *56*, 2640–2644.
[55] A. Nuthanakanti, I. Ahmed, S. Y. Khatik, K. Saikrishnan, S. G. Srivatsan, *Nucleic Acids Res.* **2019**, *47*, 6059–6072.
[56] P. Ghosh, H. M. Kropp, K. Betz, S. Ludmann, K. Diederichs, A. Marx, S. G. Srivatsan, *J. Am. Chem. Soc.* **2022**, *144*, 10556–10569.
[57] H. Chen, S. Viel, F. Ziarelli, L. Peng, *Chem. Soc. Rev.* **2013**, *42*, 7971–7982.
[58] A. Boeszoermenyi, B. Ogórek, A. Jain, H. Arthanari, G. Wagner, *J. Biomol. NMR* **2020**, *74*, 365–379.
[59] S. Manna, D. Sarkar, S. G. Srivatsan, *J. Am. Chem. Soc.* **2018**, *140*, 12622–12633.
[60] S. Roy, P. Majee, S. Sudhakar, S. Mishra, J. Kalia, P. I. Pradeepkumar, S. G. Srivatsan, *Chem. Sci.* **2024**, *15*, 7982–7991.
[61] M. Himmelstoß, K. Erharter, E. Renard, E. Ennifar, C. Kreutz, R. Micura, *Chem. Sci.* **2020**, *11*, 11322–11330.
[62] H.-L. Bao, T. Ishizuka, T. Sakamoto, K. Fujimoto, T. Uechi, N. Kenmochi, Y. Xu, *Nucleic Acids Res.* **2017**, *45*, 5501–551.
[63] W. A. Wee, J. H. Yum, S. Hirashima, H. Sugiyama, S. Park, *RSC Chem. Biol.* **2021**, *2*, 876–882.
[64] S. Y. Khatik, S. Sudhakar, S. Mishra, J. Kalia, P. I. Pradeepkumar, S. G. Srivatsan, *Chem. Sci.* **2023**, *14*, 5627–5637.
[65] A. Olszewska, R. Pohl, M. Hocek, *J. Org. Chem.* **2017**, *82*, 11431–11439.
[66] B. J. Dow, S. S. Malik, A. C. Drohat, *J. Am. Chem. Soc.* **2019**, *141*, 4952–4962.
[67] M. R. Baranowski, M. Warminski, J. Jemielity, J. Kowalska, *Nucleic Acids Res.* **2020**, *48*, 8209–8224.
[68] Q. Li, M. Trajkovski, C. Fan, J. Chen, Y. Zhou, K. Lu, H. Li, X. Su, Z. Xi, J. Plavec, C. Zhou, *Angew. Chem. Int. Ed.* **2022**, *61*, e202201848.
[69] C. Wang, G. Xu, X. Liu, L. Jiang, X. Zhou, M. Liu, C. Li, *J. Am. Chem. Soc.* **2024**, *146*, 4741–4751.
[70] P. Ménová, H. Cahová, M. Plucnara, L. Havran, M. Fojta, M. Hocek, *Chem. Commun.* **2013**, *49*, 4652–4654.
[71] M. L. Winz, E. C. Linder, T. André, J. Becker, A. Jäschke, *Nucleic Acids Res.* **2015**, *43*, e110.
[72] B. H. Le, V. T. Nguyena, Y. J. Seo, *Chem. Commun.* **2019**, *55*, 2158–2161.
[73] A. J. Berdis, *Chem. Rev.* **2009**, *109*, 2862–2879.
[74] J. Hohlbein, L. Aigrain, T. D. Craggs, O. Bermek, O. Potapova, P. Shoolizadeh, N. D. F. Grindley, C. M. Joyce, A. N. Kapanidis, *Nat. Commun.* **2013**, *4*, 2131.
[75] K. Betz, D. A. Malyshev, T. Lavergne, W. Welte, K. Diederichs, T. J. Dwyer, P. Ordoukhanian, F. E. Romesberg, A. Marx, *Nat. Chem. Biol.* **2012**, *8*, 612–614.
[76] Q. Du, N. Carrasco, M. Teplova, C. J. Wilds, M. Egli, Z. Huang, *J. Am. Chem. Soc.* **2002**, *124*, 24–25.
[77] C. Höbartner, R. Rieder, C. Kreutz, B. Puffer, K. Lang, A. Polonskaia, A. Serganov, R. Micura, *J. Am. Chem. Soc.* **2005**, *127*, 12035–12045.
[78] J. Sheng, J. Gan, A. S. Soares, J. Salon, Z. Huang, *Nucleic Acids Res.* **2013**, *41*,10476–10487.
[79] Y. Li, Y. Kong, S. Korolev, G. Waksman, *Protein Sci.* **1998**, *7*, 1116–1123.
[80] S. Obeid, H. Bußkamp, W. Welte, K. Diederichs, A. Marx, *J. Am. Chem. Soc.* **2013**, *135*, 15667–15669.
[81] J. A. Olsen, D. W. Banner, P. Seiler, H. Fischer, T. Tschopp, U. Obst-Sander, M. Kansy, K. Mueller, F. Diederich, *Org. Biol. Chem.* **2004**, *2*, 1339–1352.
[82] D. O'Hagan, *Chem. Soc. Rev.* **2008**, *37*, 308–319.
[83] S. Moran, R. X.-F. Ren, E. T. Kool, *Proc. Natl. Acad. Sci. USA* **1997**, *94*, 10506–10511.
[84] E. T. Kool, H. O. Sintim, *Chem. Commun.* **2006**, 3665–3675.
[85] G. T. Hwang, A. M. Leconte, F. E. Romesberg, *ChemBioChem* **2007**, *8*, 1606–1611.
[86] H. M. Kropp, K. Betz, J. Wirth, K. Diederichs, A. Marx, *PLoS One* **2017**,*12*, e0188005.
[87] A. A. Henry, A. G. Olsen, S. Matsuda, C. Yu, B. H. Geierstanger, F. E. Romesberg, *J. Am. Chem. Soc.* **2004**, *126*, 6923–6931.
[88] S. K. Jarchow-Choy, A. T. Krueger, H. Liu, J. Gao, E. T. Kool, *Nucleic Acids Res.* **2011**, *39*, 1586–1594.

Manuscript received: July 29, 2024
Accepted manuscript online: October 20, 2024
Version of record online: November 22, 2024